

# Electrostatic Strengths of Salt Bridges in Thermophilic and Mesophilic Glutamate Dehydrogenase Monomers

Sandeep Kumar,<sup>1</sup> Buyong Ma,<sup>2</sup> Chung-Jung Tsai,<sup>2</sup> and Ruth Nussinov<sup>1,3\*</sup>

<sup>1</sup>Intramural Research Support Program, SAIC Frederick, National Cancer Institute, Frederick Cancer Research and Development Center, Laboratory of Experimental and Computational Biology, Frederick, Maryland

<sup>2</sup>Laboratory of Experimental and Computational Biology, NCI-FCRDC, Frederick, Maryland

<sup>3</sup>Sackler Institute of Molecular Medicine, Sackler School of Medicine, Tel Aviv University, Tel Aviv, Israel

**ABSTRACT** Here we seek to understand the higher frequency of occurrence of salt bridges in proteins from thermophiles as compared to their mesophile homologs. We focus on glutamate dehydrogenase, owing to the availability of high resolution thermophilic (from *Pyrococcus furiosus*) and mesophilic (from *Clostridium symbiosum*) protein structures, the large protein size and the large difference in melting temperatures. We investigate the location, statistics and electrostatic strengths of salt bridges and of their networks within corresponding monomers of the thermophilic and mesophilic enzymes. We find that many of the extra salt bridges which are present in the thermophilic glutamate dehydrogenase monomer but absent in the mesophilic enzyme, form around the active site of the protein. Furthermore, salt bridges in the thermostable glutamate dehydrogenase cluster within the hydrophobic folding units of the monomer, rather than between them. Computation of the electrostatic contribution of salt bridge energies by solving the Poisson equation in a continuum solvent medium, shows that the salt bridges in *Pyrococcus furiosus* glutamate dehydrogenase are highly stabilizing. In contrast, the salt bridges in the mesophilic *Clostridium symbiosum* glutamate dehydrogenase are only marginally stabilizing. This is largely the outcome of the difference in the protein environment around the salt bridges in the two proteins. The presence of a larger number of charges, and hence, of salt bridges contributes to an electrostatically more favorable protein energy term. Our results indicate that salt bridges and their networks may have an important role in resisting deformation/unfolding of the protein structure at high temperatures, particularly in critical regions such as around the active site. *Proteins* 2000;38:368–383.

Published 2000 Wiley-Liss, Inc.<sup>†</sup>

**Key words:** thermostability; salt bridge; melting temperature; electrostatics; glutamate dehydrogenase

## INTRODUCTION

In folded proteins, a pair of neighboring, oppositely charged residues often interact to form salt bridges. Salt bridges have important roles in protein structure and

function e.g., oligomerization, molecular recognition, allosteric regulation, domain motions and cooperativity in protein folding.<sup>1–5</sup> One would, then, expect the salt bridges to have stabilizing contributions toward the folded, native conformations of proteins. However, theoretical as well as experimental estimates of the electrostatic strengths of salt bridges vary significantly. These range from being stabilizing,<sup>5–9</sup> to being insignificant or small,<sup>10–12</sup> to being destabilizing.<sup>13–16</sup> It has also been suggested that formation of buried salt bridges might be a slow step in protein folding.<sup>17</sup> An early calculation by Honig and Hubbell<sup>18</sup> estimated that the cost of transferring a salt bridge from water to the protein environment is approximately 10–16 Kcal/mol. This large desolvation penalty due to the burial of polar and charged groups in the protein interior (low dielectric environment) during protein folding and binding, is generally not recovered by favorable interactions in the folded/bound states.<sup>15,16</sup>

Proteins from thermophilic organisms, which are functional at high temperatures, are necessarily particularly stable. Several reasons have been suggested to account for their higher stability.<sup>19</sup> To study the contribution of each potential factor, a comparative analysis of 18 nonredundant families which contain pairs of high resolution structures of proteins from both thermophilic and mesophilic organisms has been carried out. The results have indicated that both mesophile-thermophile homologous protein pairs have similar hydrophobicities, compactness, oligomeric states, main chain-main chain and main chain-side chain hydrogen bonds. On the other hand, the number of salt bridges increases for several thermophilic proteins.<sup>20</sup> Consistently, Yip et al.<sup>21</sup> have also observed a correlation between salt bridges and thermostabilities of glutamate dehydrogenases, isolated from several thermophilic and mesophilic organisms. Hence, there arises an apparent paradox: On the one hand salt bridges have been shown to frequently destabilize proteins. On the other hand, salt bridges are observed to be more frequent in thermophilic proteins than in their mesophilic homologs. Furthermore, whereas other structural parameters such as hydrophobicity, compactness, and oligomerization have been proposed

\*Correspondence to: Ruth Nussinov, SAIC Frederick NCI-FCRF Building 469, room 151, Frederick, MD 21702.  
E-mail: ruthn@ncifcrf.gov

Received 24 May 1999; Accepted 8 October 1999

to substantially contribute to stabilize proteins from thermophiles, current available data suggest that only salt bridges show a consistent increase in proteins with high  $T_m$  values. The obvious immediate question that comes to mind is, then, if salt bridges are destabilizing, why do they occur frequently in thermophiles?

Hydration free energies of amino acids change with temperature. The temperature dependence of hydration free energies is due to a decrease in the dielectric constant of water and the contribution of entropic effects with the increase in temperature.<sup>22,23</sup> These studies on the effects of temperature on protein hydration, and the estimates of the free energies of folding of the proteins, indicate a reduced desolvation penalty for salt bridges at high temperatures. This may explain the observed increase in the number of salt bridges in the hyperthermophiles.<sup>23</sup> Recently, Xiao and Honig<sup>24</sup> have computed the electrostatic contributions to protein stability for four hyperthermophilic proteins and their mesophilic homologs. They find that hyperthermophilic proteins have greater contributions from electrostatic interactions than their mesophilic homologs. However, how individual salt bridges overcome the desolvation penalties in the hyperthermophilic proteins is still an open question.

Here we carry out computational studies of the free energy changes upon salt bridge formation in glutamate dehydrogenase from thermophiles and from mesophiles. Glutamate dehydrogenase (GDH), which catalyzes the reversible oxidative deamination of L-glutamate to 2-oxoglutarate and ammonia using  $\text{NAD}^+$  or  $\text{NADP}^+$  as cofactor, accounts for 20% of the total cell protein in the archaeon *Pyrococcus furiosus*.<sup>25</sup> *Pyrococcus furiosus* glutamate dehydrogenase (PfGDH) is extremely thermostable, with a half life of 12 hours at 100°C.<sup>26</sup> Its melting temperature ( $T_m$ ) has been reported to be 113°C.<sup>27</sup> The mesophilic *Clostridium symbiosum* glutamate dehydrogenase (CsGDH) shares 34% sequence identity with PfGDH. In both organisms, biochemically active GDH is a homohexamer. Three dimensional structures for both GDHs are available<sup>25,28,29</sup> and are highly similar.<sup>20</sup> However, in contrast to PfGDH, CsGDH has a half life of only 20 minutes at 52°C.<sup>25</sup> Its melting temperature ( $T_m$ ) is 55°C.<sup>21</sup> The striking difference in the thermostability as shown by a melting temperature difference of  $\Delta T_m \sim 60^\circ\text{C}$ , accompanied by a  $\sim 70\%$  increase in the occurrence of salt bridges for the whole hexameric biological unit,<sup>20</sup> and a concomitant high sequence and structural similarity between PfGDH and CsGDH, make this thermophile-mesophile pair an ideal model for investigating the molecular basis of thermostability. Yip et al.<sup>25</sup> have shown that salt bridges and their networks are a major contributor to the stability of PfGDH. Here we assess the electrostatic energies of salt bridges within the monomers of both enzymes. In particular, we examine the contribution of each of the terms in both dehydrogenases. We observe that salt bridges and their networks make a stabilizing contribution to the thermophilic glutamate dehydrogenase (PfGDH) monomer, whereas they contribute only marginally to the stability of the mesophilic glutamate dehydrogenase (Cs-

GDH) monomer. In the thermophilic enzyme the desolvation penalty is offset largely by the cooperative, stabilizing effect of additional salt bridges, often in the form of networks. This stabilizing effect is reflected in the protein term in our calculations. Most of the additional salt bridges found in the PfGDH monomer, but not in the CsGDH monomer, are in the vicinity of the active site of the enzyme. The higher frequency of occurrence of salt bridges may contribute to resisting local deformation/melting, or unfolding, at high temperatures.

## METHODS

### Thermophile-Mesophile Protein Pair

The coordinates for the three dimensional structures of thermophilic PfGDH and its homologue mesophilic CsGDH were retrieved from Protein Data Bank (PDB).<sup>30</sup> The PDB entry file names are 1GTM (Resolution = 2.2 Å) for PfGDH and 1HRD (Resolution = 1.96 Å) for CsGDH. In both organisms, GDH exists as homohexamer. Backbones of the B chains in 1GTM and 1HRD superimpose with a root mean square deviation of 1.38 Å.

### Salt Bridges

The presence of salt bridges was inferred when Asp or Glu side-chain carbonyl oxygen atoms were found to be within a 4.0 Å distance from the nitrogen atoms in Arg, Lys and His side chains. More than one nitrogen-oxygen pair of atoms can be within 4.0 Å in a given pair of salt bridge forming residues. In such cases, the salt bridge was counted only once.

The location of residues forming salt bridges was characterized in terms of their solvent accessible area (ASA)<sup>31,32</sup> with a probe radius of 1.4 Å. The B chains of 1GTM and 1HRD were cut into different hydrophobic folding units (HFU)<sup>32</sup> and salt bridges within, as well as across, these HFUs were identified. A residue X was classified as being exposed if its ASA is above 20% of the ASA calculated for tripeptide GLY - X - GLY in an extended conformation. Otherwise, it was classified as being an internal residue.

The overall location of the salt bridge in the protein was assessed by averaging the percent ASAs of the individual residues. A salt bridge was classified as being buried in the protein core if its average ASA was  $\leq 20\%$ , otherwise it was classified as being exposed to the solvent.

Electrostatic energies were computed for salt bridges formed within the B chains of 1GTM and 1HRD.

### Computation of Electrostatic Energies of Salt Bridges

The electrostatic strength of a salt bridge was calculated relative to a computer mutation of the salt bridging side chains to their hydrophobic isosteres. This method has already been extensively used in literature.<sup>5,9,12,15,24,46</sup> The total electrostatic energy of a salt bridge,  $\Delta\Delta G_{tot}$ , was calculated by the following equation:

$$\Delta\Delta G_{tot} = \Delta\Delta G_{dolv} + \Delta\Delta G_{brd} + \Delta\Delta G_{prt}$$

where

$\Delta\Delta G_{dsolv}$  represents the unfavorable desolvation free energy penalty (desolvation penalty) incurred due to the desolvation of the salt bridge forming side chains from water (unfolded state) to the protein interior (folded state).

$\Delta\Delta G_{brd}$  represents the free energy due to the interaction between two salt bridge forming residue side chains in the folded protein.

$\Delta\Delta G_{prt}$  represents the free energy due to the interaction of salt bridge forming side-chains with the rest of the protein.

Each of the above terms were computed using continuum electrostatics. Continuum electrostatic calculations were performed with the DELPHI package developed by Honig and coworkers,<sup>33–37</sup> under INSIGHTII release 98.0. PARSE3 set of partial atomic charges and atomic radii<sup>38</sup> were used. The PARSE set allows reproduction of the experimental data for a wide range of small organic molecules and ions representing side chains of amino acids<sup>39</sup> (see DELPHI manual at MSI website <http://www.msi.com/> for a comparison). The solvent probe radius used to define the molecular surface was 1.4 Å. A 2 Å Stern layer<sup>40</sup> was applied to exclude ions from the molecular surface. The dielectric constant for the solute (protein molecule) was 4.0 and that for solvent was 80.0. The ionic strength was 0.0 M, since current implementation of DELPHI correctly computes the reaction field energies only at zero ionic strength (DELPHI manual for version 97.0 available under Insight98). Reaction field energy gives an accurate estimate of the electrostatic solvation energy (DELPHI manual). Extensive testing reported in literature (e.g., Fig. 5 in Hendsch and Tidor<sup>15</sup>) indicates that ionic strength does not affect appreciably the final values. Recently Xiao and Honig<sup>24</sup> have also shown that the differential stability between thermophilic and mesophilic proteins is unaffected by bulk salt concentration. The Poisson equation was solved using the iterative finite difference method<sup>34–36</sup> on a three-dimensional grid with a step of 0.833 Å per grid point, with an energy convergence criterion of  $1 \times 10^{-6}$  kT (kT are the units of energy in DELPHI outputs, k is Boltzmann's constant and T is absolute Temperature). This results in mapping the PfGDH trimer (1GTM) onto a cubic grid with  $245 \times 245 \times 245$  grid points. The CsGDH trimer (1HRD) has been mapped onto a cubic grid of  $249 \times 249 \times 249$  grid points. The large number of grid points indicates that the PfGDH and CsGDH trimers have been mapped onto fine grids. Due to the large size of the system under study, the positional averaging to remove the effect of grid granularity has not been carried out. The resulting errors in our calculations are negligible owing to the fine grid (small grid spacing) which used here.

In each calculation, initially the molecule occupied 50% of the grid, and the Debye-Huckel (full Coulombic) boundary conditions were applied.<sup>41</sup> The resulting grid of this rough calculation was used as boundary condition for a focused calculation in which the molecule occupied 95% of the grid. The results of the focused calculation are presented here.

DELPHI outputs the energy values in units of kT, where k is Boltzmann constant and T is temperature. The

conversion factor between kT and Kcal/mol is temperature dependent. For example, at room temperature ( $T = 298$  Kelvin),  $1 \text{ kT} = 1.3806503 \times 10^{-23} \times 298 \text{ J}$  (where J is Joule; 1 Joule = 0.239 calories). Multiplying and dividing the above equation by Avogadro's number  $6.022 \times 10^{23}$ , we get  $1 \text{ kT} = 0.592 \text{ Kcal/mol}$ . In addition to the room temperature, results can also be presented at the optimum growth temperatures of the *Pyrococcus furiosus* (100°C) and *Clostridium symbiosum* (37°C). Conversion factors corresponding to the optimal growth temperatures of the two organisms are 0.741 (*Pyrococcus furiosus*) and 0.616 (*Clostridium symbiosum*). Dielectric constant of water at 100°C is 55.51.<sup>42</sup> For PfGDH, calculations were also performed with solvent dielectric constant of 55.51. All calculations have been done at pH 7.0.

Full biochemically active PfGDH and CsGDH are homo-hexamers. Each of these contains  $\sim 50,000$  atoms. This would have generated  $\sim 10^8$  grid points. Due to the large size of these proteins and the limitations on available computer Random access memory (RAM) required for such calculations, it was difficult to use the biochemically functional hexameric models for PfGDH and CsGDH. Instead, the calculations were performed on the crystallographic asymmetric unit, i.e., the trimers whose coordinates are given in the PDB files 1GTM and 1HRD. Previous similar calculations on glutamate dehydrogenase have used only the monomers.<sup>24</sup> In each case, hydrogens were fixed, the polypeptide chains were capped, and all residues forming the salt bridges were replaced by their ionized forms using the BIOPOLYMER module of INSIGHTII release 98.0 from Molecular Simulations, Inc.

## RESULTS

### PfGDH and CsGDH Salt Bridges and Maintenance of Protein Fold at High Temperatures

Glutamate dehydrogenase is hexameric both in *Clostridium symbiosum* and in *Pyrococcus furiosus*. According to the crystallographers' assignments,<sup>28,29</sup> each subunit of CsGDH contains two domains separated by a deep cleft. The substrate, glutamate, and the cofactor,  $\text{NAD}^+$ , bind in the deep cleft between these two domains.<sup>29</sup> The first domain (domain I, residues 1–200 and 424–449) consists of the N-terminal portion of the polypeptide and directs the oligomeric assembly of the molecule. The second domain (domain II, residues 201–423) is structurally very similar to a dinucleotide binding fold and is associated with enzyme activity. Figure 1 (a) and (b) depict the corresponding monomers in the thermophilic PfGDH (B chain of 1GTM; PDB file for PfGDH) and the mesophilic CsGDH (B chain of 1HRD; PDB file for CsGDH). As the figures show, the PfGDH monomer has several salt bridges near the active site which are missing in CsGDH. The two monomers have been further cut into hydrophobic folding units (HFU) using the algorithm of Tsai and Nussinov.<sup>32</sup> The B chain in 1GTM has four hydrophobic folding units, while the B chain of 1HRD has five. The residues belonging to each of the HFUs are listed in Table I and depicted in Figure 2. Also shown are the locations of the salt bridges in the two monomers (Fig. 2). A comparison of the salt



**TABLE I. Hydrophobic Folding Units in Monomers of *Pyrococcus furiosus* and *Clostridium symbiosum* Glutamate Dehydrogenases<sup>†</sup>**

HFU	Number of residues	Compactness	Hydrophobicity	Isolatedness (%)	Number of segments	Residue list
B chain in 1GTM						
1	48	1.44	0.71	0.16	1	240–287
2	151	1.58	0.80	0.17	1	33–183
3	165	1.69	0.79	0.17	2	184–239; 288–396
4	53	1.50	0.69	0.23	2	3–32; 397–419
1GTM-B	417	1.85	0.85	0.0	1	3–419
B chain in 1HRD						
1	128	1.56	0.81	0.13	2	54–107; 122–195
2	58	1.49	0.73	0.18	1	255–312
3	53	1.50	0.68	0.21	1	1–53
4	55	1.46	0.73	0.23	1	313–367
5	76	1.58	0.71	0.25	2	113–121; 368–434
Not assigned to any HFU						108–112; 196–254; 435–449
1HRD-B	449	1.95	0.84	0.0	1	1–449
Crystallographer's assignment for a subunit in 1HRD						
Domain I	226					1–200; 424–449
Domain II	223					201–423

<sup>†</sup>HFU stands for hydrophobic folding units.<sup>32</sup> 1GTM and 1HRD are the names of PDB files containing the crystal structures of glutamate dehydrogenase from *Pyrococcus furiosus* and *Clostridium symbiosum* respectively. For definitions of compactness, hydrophobicity and isolatedness, see Tsai and Nussinov.<sup>32</sup>

bridge locations in the two monomers shows that PfGDH has a larger number of salt bridges in the region corresponding to domain II. These observations indicate that the additional salt bridges have a role in maintaining the integrity of the active site at high temperatures.

Biochemically active hexamers of PfGDH and CsGDH contain 168 and 107 salt bridges respectively (criteria are listed in Methods). When normalized by the number of residues in each hexamer, this represents a ~70% increase in the frequency of salt bridges in PfGDH over CsGDH. 128 (76.2%) out of the 168 salt bridges in the PfGDH are formed within the six subunits and 40 (23.8%) salt bridges are formed across the subunit interfaces. In comparison, 75 (70.1%) out of 107 salt bridges in CsGDH are formed within the subunits and 32 (29.9%) salt bridges are formed across the subunit interfaces. Salt bridges and their networks across subunit interfaces have been studied earlier.<sup>21,25</sup> Here we focus on salt bridges that are formed within GDH monomers. The B chain of 1GTM contains 40 salt bridges, while that of 1HRD contains only 20 salt bridges. Table II (a) and (b) list the salt bridge-forming residues in the B chains of 1HRD and 1GTM, respectively, along with their accessible surface areas (ASA). The accessible surface areas are listed for these residues in the trimeric forms of GDHs (as in the crystal asymmetric unit) as well as in the whole biochemically active hexamers. Most of the salt bridges in the GDHs are solvent exposed (average ASA > 20%). Furthermore, Table II(a) and (b)

show that most of the salt bridges are formed within the hydrophobic folding units: 37 out of 40 salt bridges in the PfGDH are formed within the HFUs, while in the case of CsGDH 15 out of 20 salt bridges are formed within the HFUs. Additionally, the B chain of 1GTM (PfGDH monomer) is more compact as compared to the B chain of 1HRD (CsGDH monomer) (Table I). Furthermore, the B chain of 1GTM contains eight salt bridge networks, two triads, three tetrads, two pentads and one hexad (Table II(b)). In contrast, the B chain of 1HRD contains only two triads and a tetrad (Table II(a)).

Fig. 1. (Overleaf.) Diagrams showing C<sup>α</sup> trace, active site, and salt bridge-forming residues in a subunit of glutamate dehydrogenase from the (a) hyperthermophilic archaeobacterium *Pyrococcus furiosus* (chain B in 1GTM) and (b) mesophilic gram positive bacterium *Clostridium symbiosum* (chain B in 1HRD). All the heavy atoms are shown for salt bridge-forming as well as for active-site residues. Active-site residues are shown with CPK representation. The conserved active site Lys which participates in salt bridge network formation as well as in enzyme activity is shown in red. Other active site residues are in green. Residues with side-chain atoms shown in red are the positively charged residues (Arg, Lys, or His) while the residues with side-chain atoms shown in blue are the negatively charged residues (Glu or Asp), in ball-and-stick representation. C<sup>α</sup> atoms of the salt bridge-forming residues are shown in black. Thermophilic glutamate dehydrogenase has several additional salt bridges in the neighborhood of the active site as compared to the mesophilic glutamate dehydrogenase. Residues in the active site of *Pyrococcus furiosus* glutamate dehydrogenase have been inferred from three dimensional structural superposition of monomers of 1GTM and 1HRD, using the method described by Tsai et al.<sup>43</sup>

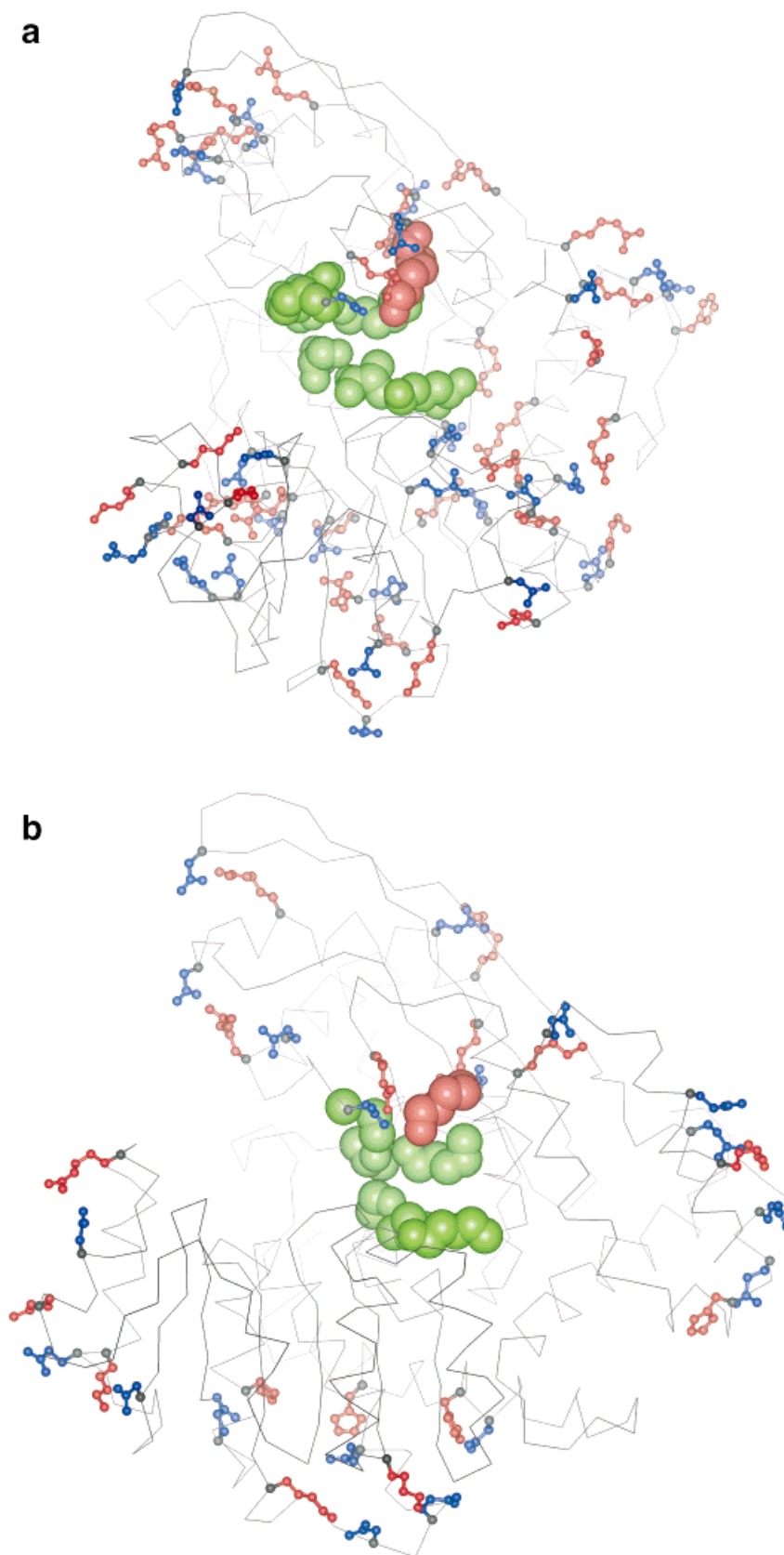


Figure 1. (Legend on previous page.)

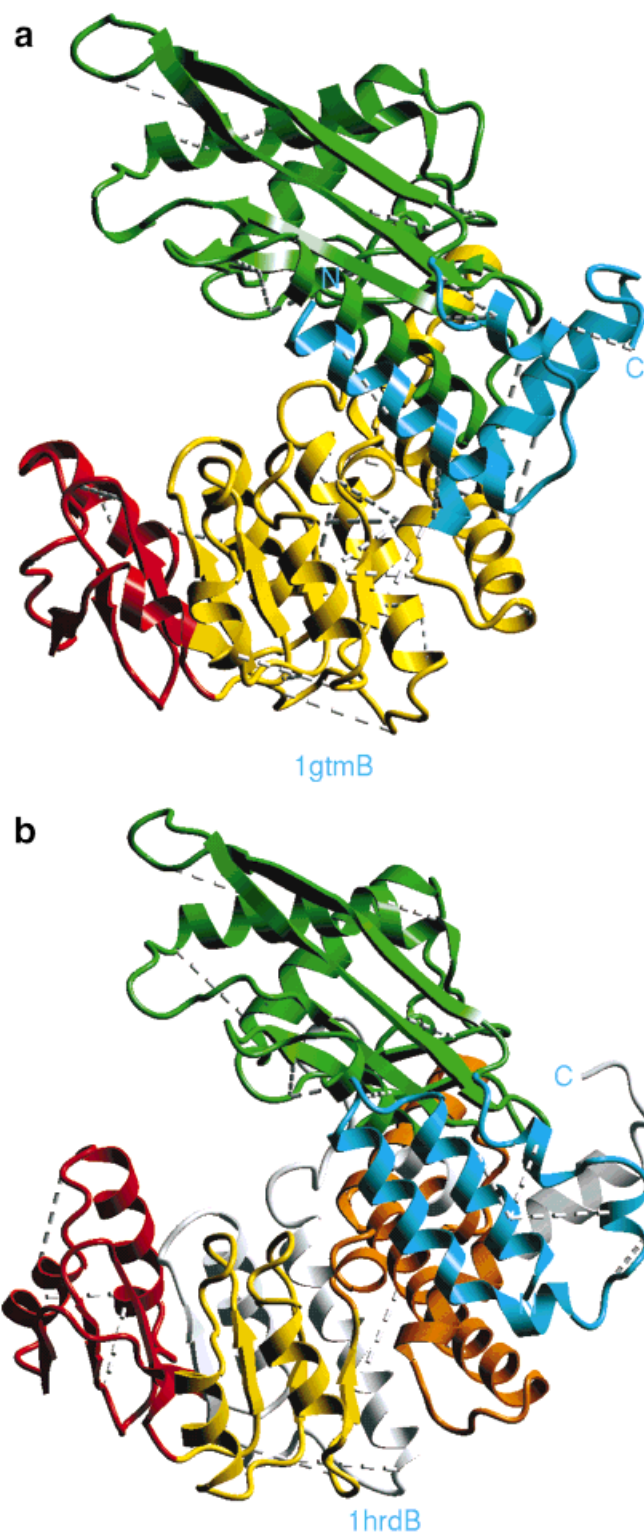


Figure 2. (Legend on following page.)

TABLE II(A). Salt Bridges in *Clostridium symbiosum* Glutamate Dehydrogenase (Chain B of 1HRD)<sup>†</sup>

Salt bridge	ASA trimer		ASA hexamer		Salt bridge type	HFU
	ASA <sub>1</sub> (%)	ASA <sub>2</sub> (%)	ASA <sub>1</sub> (%)	ASA <sub>2</sub> (%)		
<b>R 6 - E 10</b>	38.5	47.1	38.5	47.1	E	3,3
<b>R 6 - E 43</b>	38.5	42.3	38.5	42.3	E	3,3
R 6 - E 49	38.5	20.6	38.5	14.4	E	3,3
<b>E 18 - K104</b>	12.4	2.5	12.4	2.5	B	3,1
<b>H 39 - E 41</b>	14.8	36.3	14.8	36.3	E	3,3
D 67 - R142	49.9	25.0	43.0	11.5	E	1,1
<b>R 78 - D160</b>	0.0	0.0	0.0	0.0	B	1,1
<b>R 93 - D165</b>	20.5	31.2	20.5	31.2	E	1,1
<b>K125 - D165</b>	5.4	31.2	5.4	31.2	B	1,1
<b>D137 - R171</b>	50.7	42.9	50.7	40.8	E	1,1
E150 - R153	24.5	56.9	0.0	29.3	B	1,1
<b>R171 - E172</b>	42.9	3.9	40.8	3.9	E	1,1
<b>E218 - H403</b>	21.0	28.5	21.0	27.6	E	-,5
<b>E224 - K340</b>	25.2	25.4	25.2	25.4	E	-,4
<b>D226 - K231</b>	33.4	16.0	33.4	16.0	E	-, -
<b>K248 - E251</b>	4.3	64.5	4.3	64.5	E	-, -
<b>D268 - K277</b>	0.0	9.3	0.0	9.3	B	2,2
<b>E276 - K298</b>	57.6	47.8	57.6	47.8	E	2,2
<b>R289 - D294</b>	59.5	7.9	59.5	7.7	E	2,2
<b>H410 - D411</b>	0.4	48.6	0.4	48.6	E	5,5

<sup>†</sup>Each salt bridge is defined by the residues forming it. The residues are denoted using single letter code for amino acids. ASA stands for accessible surface area.<sup>31,32</sup> Salt bridge types are denoted by symbols B and E. B indicates a buried salt bridge and E indicates an exposed salt bridge. The definitions of buried and exposed salt bridges are given in the Methods section. Assignment of residues into various HFUs is given in Table I. — indicates that the residue can not be assigned to any HFU. ASAs for salt bridge-forming residues are given in the trimeric (crystal asymmetric unit) and hexameric (biochemically functional form) states of glutamate dehydrogenase. Salt bridges with similar ASAs in the trimeric and hexameric states are shown in bold. Continuum electrostatic calculations were performed only for the salt bridges that are shown in bold.

The glutamate binding moiety in glutamate dehydrogenase contains three conserved Lys residues. One of these three lysines has been implicated in the activity of the enzyme.<sup>28</sup> In CsGDH, this lysine (K125) also participates in the formation of a salt bridge triad (R93 - D165 - K125) near the active site. We have identified the active site residues in PfGDH using a computer vision-based structure comparison method described by Tsai et al.<sup>43</sup> The corresponding Lys residue in PfGDH, K104, also participates in a salt bridge tetrad (E77 - R72 - D144 - K104) near the active site. Thus, the salt bridge network which is directly associated with the active site is more extensive in the thermophile. Furthermore, electrostatic energy calculations (described below and in Table III) indicate that the salt bridges involved in these active site-associated networks have greater stabilities in PfGDH. This observation further substantiates our conclusion that an increase in the number of salt bridges and their networks in PfGDH is essential for enzyme activity at high temperatures.

### Electrostatic Energies of Salt Bridges Within Monomers of PfGDH and CsGDH

We have performed an electrostatic analysis of the energetics of salt bridge formation in the B subunits of 1GTM (PfGDH) and 1HRD (CsGDH) using the continuum model in the DELPHI package.<sup>33–37</sup> The concepts behind each term are presented in a schematic diagram in Figure 3. With a more rigorous definition, we should have used the whole biochemically active hexamer for the calculations. However, the computer random access memory (RAM)-intensive nature of each DELPHI calculation, combined with the large size of the protein prohibit such a large calculation (see Methods for details). Recent electrostatic calculations on glutamate dehydrogenase have used only the monomer.<sup>24</sup> However, it is desirable to use higher oligomeric forms of GDH to take into account long range electrostatic effects. As a compromise between computational difficulty and the desirability of an accurate estimate of electrostatic energies, we have used trimers (as in the crystal asymmetric unit) in our calculations. Subunit B in each trimer is surrounded by subunits A and C. We have used the B subunits of PfGDH and CsGDH in our calculations. However, this simplification still exposes us to the danger of underestimating the desolvation penalty incurred by the salt bridge forming side chains near trimer-trimer interfaces. To work around this difficulty, we have used the accessible surface area (ASA)<sup>31,32</sup> to estimate the location of salt bridge-forming residues in the trimeric and hexameric states of the glutamate dehydrogenase. If both residues which form the salt bridge have identical, or

Fig. 2. (Overleaf.) Ribbon diagrams showing the hydrophobic folding units (HFU)<sup>32</sup> in a subunit in glutamate dehydrogenase from (a) hyperthermophilic archaeobacterium *Pyrococcus furiosus* (Chain B in 1GTM) and (b) mesophilic gram positive bacterium *Clostridium symbiosum* (chain B in 1HRD). Ribbon colored white indicates residues which are unassigned to a specific HFU in the case of the mesophilic glutamate dehydrogenase (1HRD) (Table I). Broken lines indicate the location of salt bridges in the two proteins. For sake of simple representation, C<sup>α</sup> atoms of the residues forming the salt bridges have joined by the broken lines. Note the formation of salt bridge networks in the thermophilic glutamate dehydrogenase in the region corresponding to the unassigned region in the mesophilic protein.

TABLE II(B). Salt Bridges in *Pyrococcus furiosus* Glutamate Dehydrogenase (Chain B of 1GTM)<sup>†</sup>

Salt bridge	ASA trimer		ASA hexamer		Salt bridge type	HFU
	ASA <sub>1</sub> (%)	ASA <sub>2</sub> (%)	ASA <sub>1</sub> (%)	ASA <sub>2</sub> (%)		
<b>E 7 - K 11</b>	46.1	55.0	46.1	55.0	E	4,4
<b>R 15 - D397</b>	38.7	2.9	38.7	2.9	E	4,4
E 25 - H419	36.0	72.5	8.2	57.4	E	4,4
E 28 - K 31	35.2	16.5	28.8	16.5	E	4,4
E 28 - K 32	35.2	56.5	28.8	30.9	E	4,4
R 35 - E138	30.0	27.8	1.3	0.3	B	2,2
D 46 - R121	53.8	29.6	53.8	15.1	E	2,2
<b>R 57 - D139</b>	0.0	0.0	0.0	0.0	B	2,2
R 64 - D 97	22.5	33.1	4.6	33.1	B	2,2
<b>R 72 - E 77</b>	13.1	1.3	13.1	1.3	B	2,2
<b>R 72 - D144</b>	13.1	32.7	13.1	32.7	E	2,2
<b>D 97 - K379</b>	33.1	43.1	33.1	43.1	E	2,3
<b>K104 - D144</b>	5.9	32.7	5.9	32.7	B	2,2
R117 - E120	46.9	17.1	16.2	1.9	B	2,2
E120 - R124	17.1	21.3	1.9	13.3	B	2,2
R124 - D157	21.3	34.9	13.3	3.2	B	2,2
R124 - E158	21.3	6.2	13.3	0.2	B	2,2
R128 - E158	65.9	6.2	21.2	0.2	B	2,2
<b>E188 - R192</b>	6.9	7.4	6.9	7.4	B	3,3
<b>E188 - R370</b>	6.9	31.6	6.9	31.6	B	3,3
<b>R192 - D234</b>	7.4	56.6	7.4	56.6	E	3,3
<b>R199 - E200</b>	21.5	0.0	21.5	0.0	B	3,3
<b>R199 - D374</b>	21.5	21.3	21.5	21.3	E	3,3
<b>E200 - K203</b>	0.0	54.0	0.0	54.0	E	3,3
<b>D208 - K213</b>	90.4	14.8	90.4	14.8	E	3,3
<b>K229 - E233</b>	22.1	60.6	22.1	60.6	E	3,3
<b>K229 - D258</b>	22.1	29.2	22.1	29.2	E	3,1
<b>D244 - K264</b>	7.6	19.1	6.8	19.1	B	1,1
<b>E259 - K262</b>	46.1	48.8	46.1	48.8	E	1,1
<b>K271 - D272</b>	37.1	59.2	37.1	59.2	E	1,1
<b>D290 - K312</b>	14.9	47.6	14.9	47.5	E	3,3
<b>D307 - K333</b>	53.8	47.4	53.8	46.7	E	3,3
<b>E316 - R396</b>	0.0	8.8	0.0	8.8	B	3,3
<b>D327 - H394</b>	6.4	6.7	6.4	6.7	B	3,3
<b>D327 - R396</b>	6.4	8.8	6.4	8.8	B	3,3
<b>D340 - R396</b>	1.7	8.8	1.7	8.8	B	3,3
<b>E371 - K375</b>	49.6	61.9	49.6	58.3	E	3,3
<b>K379 - D383</b>	43.1	21.5	43.1	21.5	E	3,3
<b>D383 - R406</b>	21.5	17.6	21.5	17.2	B	3,4
<b>E390 - K391</b>	70.0	41.1	70.0	41.1	E	3,3

See Table II(A) footnotes.

nearly identical, accessibilities in the trimeric and the hexameric states, we assume that the environment of the salt bridge is unaffected by the use of a protein trimer as compared to the hexamer, and the estimates of salt bridge strengths obtained by our calculations are reasonably accurate. Table II(a) and (b) list the salt bridge forming residues in the B chains of 1HRD and 1GTM respectively, along with their ASAs in the trimeric as well as in the hexameric forms of GDHs. Both residue-partners participating in 29 out of the 40 salt bridges in chain B of 1GTM have similar ASAs when computed in the trimeric and in the hexameric states. These can be considered to have similar extents of burial/exposure, i.e., similar locations with respect to their neighborhoods in the trimeric and the hexameric states. In the case of CsGDH, the chain B of 1HRD has 17 salt bridges where both residues have nearly

identical ASAs in the trimeric and hexameric states. For a salt bridge where one or both residues have different ASAs in the trimeric and the hexameric forms, either one or both residues occur at, or near a trimer interface. We did not perform calculations on such salt bridges. Since we are still able to retain most of the salt bridges in our calculations and the criteria for rejection of the salt bridges (3/20 for CsGDH and 11/40 for PfGDH) are uniform, the results of our calculations are not biased due to these constraints.

Table III(a) and (b) present the results of the salt bridge calculations for CsGDH and PfGDH. The free energy of each salt bridge can be partitioned into three components: the desolvation energy penalty,  $\Delta\Delta G_{dolv}$ , salt bridge side chains interaction,  $\Delta\Delta G_{brd}$ , and salt bridge-protein interaction,  $\Delta\Delta G_{prt}$ . The physical concepts behind each of these terms are detailed in Methods.  $\Delta\Delta G_{tot}$  is the sum of the



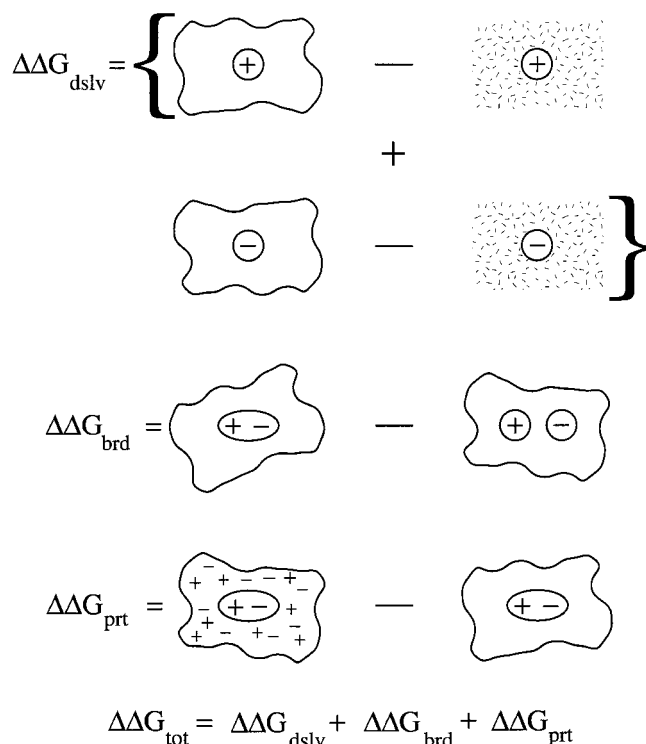


Fig. 3. A schematic diagram of the concepts behind each energy term computed to estimate electrostatic energy of a salt bridge. Side chains of the residues forming a salt bridge are shown by + and - symbols indicating their acidic or basic nature. Circles represent individual residue side chains and ovals represent the salt bridge. Dense broken lines around the side chains indicate water medium ( $\epsilon = 80$ ), while the irregular shapes around the side chains and salt bridge indicate protein interior medium ( $\epsilon = 4$ ). + and - symbols outside the salt bridge indicate other charges present in the protein.  $\Delta\Delta G_{\text{dslv}}$  is the desolvation energy penalty incurred by bringing a pair of side chains forming a salt bridge from high dielectric water medium in the unfolded protein to the low dielectric interior of the folded protein.  $\Delta\Delta G_{\text{brd}}$  is the energy of interaction between two side chains within the salt bridge.  $\Delta\Delta G_{\text{prt}}$  is the interaction of the salt bridge with the charges present in the rest of the protein.  $\Delta\Delta G_{\text{tot}}$  is the total electrostatic energy of the salt bridge obtained by summing the above three energy terms. Details regarding each energy term, are in the Methods. For PfGDH, calculations were also performed with water dielectric constant of 55.51.

three terms. The results presented in these tables are in terms of Kcal/mol at the respective temperatures of optimum growth for *Pyrococcus furiosus* and *Clostridium symbiosum*. The average values of the energy terms are also presented for room temperature to facilitate direct comparison. The thermophilic monomer has only two (out of 29 (6.9%)) destabilizing salt bridges. On the other hand, the mesophilic monomer has 6 out of 17 (35.3%) salt bridges which are destabilizing. Further, for six salt bridges in the 1HRD mesophile, the total free energy change is on the order of -1 Kcal/mol. On average, the unfavorable desolvation energy penalty is compensated by the bridge and protein energy terms by only a small margin in the salt bridges in the mesophilic monomer (average total free energy change = -1.5 Kcal/mol). As a result, these salt bridges have little stabilizing electrostatic effect. In contrast, the desolvation penalty is more

than compensated by the bridge and protein energy terms in the salt bridges of the thermophilic monomer (average total free energy change = -5.5 Kcal/mol). Several salt bridges, particularly those forming part of networks, are highly stabilizing. On average,  $\Delta\Delta G_{\text{brd}}$  and  $\Delta\Delta G_{\text{prt}}$  have similar magnitudes in PfGDH. This suggests that the interaction of charged side chains in the salt bridge-forming residues with the rest of protein, is almost as significant as the interaction of these side chains with each other. As a result, the salt bridges have a strong stabilizing electrostatic contribution toward protein thermostability. We note that the results presented here are for individual salt bridges (irrespective of their isolated or networked state). Recently, Xiao and Honig<sup>24</sup> have studied five out of eight ion pair networks in a PfGDH monomer.

The hydration free energies of amino acids are temperature dependent, and hence should also be considered in estimating the energies of salt bridges at high temperatures. The temperature dependence of the hydration free energies is due to a decrease in the dielectric constant of water and an increase in the atomic radii with an increase in temperature.<sup>22</sup> The calculated and experimental changes in the hydration free energies of amino acids are typically on the order of 1 Kcal/mol for an increase in temperature from 25°C to 100°C (Table III in Elcock and McCammon<sup>22</sup>). Elcock and McCammon<sup>22</sup> have used the Born model to describe the electrostatic solvation of spherical ions. The hydration free energy as defined there includes non-electrostatic terms as well. On the other hand, our calculations are limited to electrostatics. In our calculations, we have used point charges, rather than spherical charges. In a second set of calculations, described below, we account for a reduction in the dielectric constant of water at high temperature, along with the conversion factor. The dielectric constant of water (solvent) decreases to 55.51 at 100°C.<sup>42</sup> Table III(c) presents the results of the computations of the free energies of salt bridges in PfGDH with a solvent dielectric constant of 55.51. The reduction in water dielectric affects the bridge and protein terms, along with the desolvation term. However, while the changes in the desolvation and protein terms are negligible, the bridge term improves by an average of 0.86 Kcal/mol. This improvement may be due to a reduced electrostatic screening of the interactions between the charged side chains by the water. On average, the salt bridges in PfGDH become more stabilizing, with the average free energy change decreasing from -5.52 Kcal/mol to -6.49 Kcal/mol. These results complement those of Elcock,<sup>23</sup> which indicate that the salt bridges in the hyperthermophiles may be highly stabilizing. Recently, similar indications have also come from the study of Xiao and Honig.<sup>24</sup>

### Comparison of Energy Terms in PfGDH and CsGDH Salt Bridges

Figure 4 presents a comparison of the contributions of the energy terms to salt bridge stability in the thermophilic-mesophilic protein pair. All three energy terms in the mesophilic protein salt bridges have smaller magnitudes. This is consistent with the average values for the

TABLE III(A). Energies of Salt Bridges in CsGDH (B Chain of 1HRD)<sup>†</sup>

Salt bridge	ASA <sub>av</sub> (%)	$\Delta\Delta G_{tot}$ (Kcal/mole)	$\Delta\Delta G_{dolv}$ (Kcal/mole)	$\Delta\Delta G_{brd}$ (Kcal/mole)	$\Delta\Delta G_{prt}$ (Kcal/mole)
R 6 - E 10	42.8	+0.099	2.986	-1.139	-1.749
R 6 - E 43	40.4	-1.144	3.162	-2.059	-2.247
E 18 - K104	7.5	+1.514	10.751	-7.346	-1.892
H 39 - E 41	25.6	-1.387	6.075	-2.909	-4.554
R 78 - D160	0.0	-6.588	26.376	-28.380	-4.584
R 93 - D165	25.9	-7.290	6.848	-9.961	-4.177
K125 - D165	18.3	-6.268	9.586	-5.165	-10.689
D137 - R171	45.7	-0.311	4.935	-2.284	-2.962
R171 - E172	22.4	-7.107	7.113	-6.249	-7.971
E218 - H403	22.4	+1.504	4.368	-3.786	+0.472
E224 - K340	25.3	+3.561	5.677	-2.599	+0.482
D226 - K231	24.7	-6.559	5.085	-5.350	-6.294
K248 - E251	34.4	+0.832	6.049	-2.359	-2.858
D268 - K277	4.7	-1.618	15.803	-14.001	-3.421
E276 - K298	52.7	-1.621	1.459	-1.783	-1.297
R289 - D294	33.6	-0.356	7.765	-2.573	-5.548
H410 - D411	24.5	+7.072	9.694	-4.092	+1.470
Average	26.5 ± 14.3	-1.536 ± 0.068	7.867 ± 5.856	-6.002 ± 6.657	-2.734 ± 2.598
Average at 25°C	26.5 ± 14.3	-1.476 ± 3.910	7.560 ± 5.628	-5.768 ± 6.398	-2.627 ± 2.497

<sup>†</sup>ASA<sub>av</sub> indicates average accessible surface area of the two residues forming a salt bridge in the hexameric state of glutamate dehydrogenase.  $\Delta\Delta G_{tot}$  refers to the total electrostatic free energy of the salt bridge.  $\Delta\Delta G_{dolv}$  indicates the desolvation energy penalty incurred by the salt bridge.  $\Delta\Delta G_{brd}$  is the free energy of the interaction of salt bridge-forming side chains with each other.  $\Delta\Delta G_{prt}$  is the free energy of the interaction of salt bridge-forming side chains with the rest of the protein. Complete description of the energy terms is given in Methods. DELPHI calculations for values shown in Tables III(a) and III(b) have been performed with water dielectric constant of 80, while those for the values shown in Table III(c) have been performed with water dielectric constant of 55.51. Dielectric constant of water is 55.51 at 100°C. Energies are presented for only those salt bridges which have equivalent locations in the trimeric (crystal asymmetric unit) and hexameric (functional form) states of glutamate dehydrogenase. Averages of various energy terms at room temperature are also given in Tables III(a) and III(b) for the purpose of comparison.

three terms in Table III. Hence, even though salt bridges in the mesophilic protein pay smaller desolvation penalties, in general these are not recovered since the magnitudes of the bridge and protein energy terms are smaller as well. The shift in the contributions of the energy terms between the thermophilic and the mesophilic salt bridges can in part be explained by the difference in the conversion factors used to obtain the values in Kcal/mol for the thermophilic and mesophilic GDH. Due to this effect, a conserved salt bridge will have a greater strength in PfGDH, even if we ignore the decrease in dielectric constant of water. Nevertheless, shifts due to this difference in conversion factors are small. For example, the magnitudes of energies of the various terms will only increase by 12.5% ( $0.741 - 0.616 = 0.125$ ) for a 63°C (100–37) increase in the temperature optima between the thermophilic and mesophilic organisms. Tables III(a) and III(b) present also the average values of the energy terms at room temperature. This removes the temperature shift effects and allows a direct comparison between the energy terms for salt bridges in PfGDH and CsGDH monomers. It can be seen that all three energy terms have greater magnitudes for PfGDH monomer.

A spatially-conserved salt bridge between the subunits of the thermophilic PfGDH and the mesophilic CsGDH, has been detected by the sequence order-independent structural comparison technique,<sup>43</sup> when applied to chains B of 1GTM and of 1HRD. The conservation is further corroborated by the average ASA in the hexameric states

of 1GTM and 1HRD. This salt bridge is formed by Arg 57 and Asp 139 in the B chain of 1GTM and by Arg 78 and Asp 160 in the B chain of 1HRD. In both proteins, the residues forming this salt bridge are completely buried with their ASAs being zero. This salt bridge is very stable in both thermophilic and mesophilic GDH, with its stability being larger by 1.61 Kcal/mol (24.4%) for the thermophilic GDH. This highly stable, yet completely buried, salt bridge in GDH may appear to be an exception in light of the recent results showing that buried salt bridges are destabilizing.<sup>15–17</sup> However, cases of highly stable salt bridges buried to a similar extent have been noted earlier in Cytochrome P450 cam.<sup>9</sup> Figure 5 shows this conserved salt bridge in PfGDH and CsGDH. In this salt bridge, the N<sup>ε</sup> and N<sup>η2</sup> atoms of the Arg side chain come within hydrogen-bonding distance to O<sup>δ1</sup> and O<sup>δ2</sup> atoms in the Asp side chain. Formation of hydrogen bonds in this salt bridge may explain its stability in PfGDH and CsGDH. Table III(a), (b), and (c) illustrate that this salt bridge has a large bridge energy term which more than compensates for the high desolvation energy penalty paid due to the complete burial of the salt bridge forming residues.

### Cooperative Nature of Electrostatic Interactions

In light of these results, it behooves us to ask what causes salt bridges to be highly stabilizing in hyperthermophiles, in contrast to their counterparts in the mesophiles. The answer may lie in salt bridge networks and the cooperative nature of electrostatic interactions. Table III(a)

TABLE III(B). Energies of Salt Bridges in B Chain of 1GTM<sup>†</sup>

Salt bridge	ASA <sub>av</sub> (%)	$\Delta\Delta G_{tot}$ (Kcal/mole)	$\Delta\Delta G_{dsolv}$ (Kcal/mole)	$\Delta\Delta G_{brd}$ (Kcal/mole)	$\Delta\Delta G_{prt}$ (Kcal/mole)
E 7 - K 11	50.6	+2.395	3.970	-1.292	-0.283
R 15 - D397	20.8	-6.131	7.300	-9.805	-3.627
R 57 - D139	0.0	-7.357	32.101	-34.096	-5.362
R 72 - E 77	7.2	-8.931	16.168	-22.856	-2.243
R 72 - D144	22.9	-19.098	12.722	-4.678	-27.142
D 97 - K379	38.1	-2.459	5.646	-4.492	-3.613
K104 - D144	19.3	-4.199	9.661	-6.636	-7.224
E188 - R192	7.1	-15.086	9.965	-13.464	-11.587
E188 - R370	19.2	-13.107	9.592	-14.524	-8.176
R192 - D234	32.0	-1.384	8.920	-2.947	-7.358
R199 - E200	10.8	-8.110	13.040	-8.922	-12.227
R199 - D374	21.4	-4.690	9.588	-9.506	-4.722
E200 - K203	27.0	-6.004	8.661	-8.443	-6.221
D208 - K213	52.6	-5.265	5.160	-6.034	-4.391
K229 - E233	41.4	-10.042	4.950	-9.834	-5.157
K229 - D258	25.7	-5.927	7.887	-5.714	-8.100
D244 - K264	13.0	-6.278	16.938	-6.974	-16.241
E259 - K262	47.5	-1.972	0.108	-2.099	+0.019
K271 - D272	48.1	-4.535	0.921	-5.418	-0.038
D290 - K312	31.2	-1.939	6.265	-2.677	-5.526
D307 - K333	50.2	-3.703	2.659	-2.311	-4.051
E316 - R396	4.4	-6.729	20.492	-16.091	-11.131
D327 - H394	6.5	+10.849	17.637	-6.711	-0.077
D327 - R396	7.6	-10.537	15.574	-11.559	-14.553
D340 - R396	5.3	-13.865	16.281	-4.030	-26.116
E371 - K375	54.0	-1.093	2.233	-2.539	-0.787
K379 - D383	32.3	-2.055	7.333	-4.747	-4.641
D383 - R406	19.4	-1.507	9.382	-6.307	-4.582
E390 - K391	55.6	-1.792	1.130	-2.527	-0.396
Average	26.6 ± 17.5	-5.524 ± 5.747	9.731 ± 6.928	-8.162 ± 6.977	-7.093 ± 6.917
Average at 25°C	26.6 ± 17.5	-4.413 ± 4.591	7.774 ± 5.535	-6.521 ± 5.574	-5.667 ± 5.526

<sup>†</sup>See Table III(A) footnotes.

shows that for the mesophilic glutamate dehydrogenase (CsGDH), the interaction energy between the salt-bridging charged side chains ( $\Delta\Delta G_{brd}$ ) is considerably greater in magnitude than the interaction energy between the charged side chains and the rest of the protein ( $\Delta\Delta G_{prt}$ ). On the other hand,  $\Delta\Delta G_{brd}$  and  $\Delta\Delta G_{prt}$  have similar magnitudes in PfGDH. On average, the magnitude of  $\Delta\Delta G_{prt}$  increases by 270% in PfGDH salt bridges as compared to CsGDH salt bridges. The average  $\Delta\Delta G_{prt}$  in PfGDH is -7.395 Kcal/mol (Table III(c)) and in CsGDH it is -2.734 Kcal/mol (Table III(a)). PfGDH is particularly rich in salt bridge networks.<sup>21,25</sup> There are eight clusters of salt bridge networks in the B chain of 1GTM. We notice that several salt bridge clusters lie around the active site (Fig. 1). In total, these clusters account for 23 out of 29 salt bridges whose electrostatic energies have been discussed in the previous section. Our calculations indicate that six of these 23 salt bridges are highly stabilizing. In these salt bridges, the protein energy terms have large magnitudes. The cooperativity of the network can resist unfolding, opposing disorder. This is particularly crucial at the high temperatures at which the thermophiles live. Thus, salt bridge networks may provide a mechanism to counteract melting/unfolding. On the other hand, the salt bridge

formed between Asp 327 and His 394 in 1GTM B is highly destabilizing, even though it is part of a pentad. In this case, the contribution from the protein energy term is very small, indicating that this salt bridge lies at the edge of the network. Owing to the buried nature of this salt bridge, it incurs a high desolvation penalty which is not compensated by the bridge energy term. A salt bridge network as a whole may, however, still be destabilizing even though the individual salt bridges in the network are stabilizing.<sup>9</sup> While here we have centered only on the electrostatic strengths of individual salt bridges (networked or isolated), it is encouraging to note that three out of the five ion pair networks in the PfGDH monomer which have been studied by Xiao and Honig,<sup>24</sup> are stabilizing.

Lounnas and Wade<sup>9</sup> have studied the electrostatic stabilization of a salt link due to favorable interactions with the surrounding protein atoms. They have concluded that protein atoms within 10 Å of the center of a salt link contribute to its stability. Hence, while an extended network is the most straightforward way of gaining environmental protein stabilization, a higher concentration of charges around the salt bridge may also contribute toward this goal. Recently, deBakker et al.<sup>44</sup> have also arrived at similar conclusions through a molecular dynamics study of

TABLE III(C). Energies of Salt Bridges in B Chain of 1GTM With Water Dielectric Constant,  $\epsilon = 55.51$  at 100°C<sup>†</sup>

Salt bridge	ASA <sub>av</sub> (%)	$\Delta\Delta G_{tot}$ (Kcal/mole)	$\Delta\Delta G_{dslv}$ (Kcal/mole)	$\Delta\Delta G_{brd}$ (Kcal/mole)	$\Delta\Delta G_{prt}$ (Kcal/mole)
E 7 - K 11	50.6	+2.027	4.060	-1.725	-0.307
R 15 - D397	20.8	-7.197	7.669	-10.830	-4.067
R 57 - D139	0.0	-8.198	31.304	-34.452	-5.049
R 72 - E 77	7.2	-9.861	16.082	-23.665	-2.278
R 72 - D144	22.9	-20.748	12.983	-5.434	-28.296
D 97 - K379	38.1	-3.403	6.191	-5.559	-4.035
K104 - D144	19.3	-5.187	10.301	-7.858	-7.630
E188 - R192	7.1	-16.656	10.243	-14.348	-12.551
E188 - R370	19.2	-14.382	9.746	-15.425	-8.703
R192 - D234	32.0	-1.831	9.170	-3.749	-7.252
R199 - E200	10.8	-9.601	13.055	-9.702	-12.954
R199 - D374	21.4	-5.628	9.792	-10.443	-4.978
E200 - K203	27.0	-6.980	8.817	-9.524	-6.273
D208 - K213	52.6	-6.096	5.341	-6.907	-4.530
K229 - E233	41.4	-11.076	5.124	-10.877	-5.323
K229 - D258	25.7	-7.911	7.965	-7.302	-8.574
D244 - K264	13.0	-7.102	16.855	-7.716	-16.240
E259 - K262	47.5	-2.512	0.229	-2.758	+0.017
K271 - D272	48.1	-4.535	0.921	-5.418	-0.038
D290 - K312	31.2	-2.433	6.600	-3.370	-5.663
D307 - K333	50.2	-4.589	2.804	-2.840	-4.553
E316 - R396	4.4	-7.751	20.787	-17.100	-11.438
D327 - H394	6.5	+9.967	17.887	-7.534	-0.386
D327 - R396	7.6	-11.781	15.899	-12.759	-14.922
D340 - R396	5.3	-14.999	16.829	-4.986	-26.842
E371 - K375	54.0	-1.765	2.495	-3.292	-0.968
K379 - D383	32.3	-3.144	7.764	-5.751	-5.157
D383 - R406	19.4	-2.362	9.786	-7.178	-4.971
E390 - K391	55.6	-2.419	1.280	-3.205	-0.494
Average	26.6 ± 17.5	-6.488 ± 5.985	9.931 ± 6.818	-9.024 ± 6.962	-7.395 ± 7.121

<sup>†</sup>See Table III(A) footnotes.

salt bridges in the protein Sac7d from *Sulfolobus acidocaldarius*.

In summary, our results suggest an explanation for the increased frequency of salt bridges in PfGDH as compared to CsGDH. These also indicate the possible origin of the increased stability of the salt bridges and the advantages gained by formation of salt bridge networks in PfGDH.

## DISCUSSION

Measurements of electrostatic stability of salt bridges have been the subject of several experimental and theoretical investigations. We have followed the computational method described by Hendsch and Tidor (1994). This method involves continuum electrostatic calculations via solution of Poisson-Boltzmann equations on a three-dimensional grid around the protein containing the salt bridge(s). Our results are in good agreement with those of Hendsch and Tidor.<sup>15</sup> On a randomly selected sample of five salt bridges from their dataset, we found excellent correlations for all the energy terms, namely,  $\Delta\Delta G_{dslv}$  (linear correlation coefficient,  $r = 0.891$ ),  $\Delta\Delta G_{brd}$  ( $r = 0.973$ ),  $\Delta\Delta G_{prt}$  ( $r = 0.994$ ) and  $\Delta\Delta G_{tot}$  ( $r = 0.744$ ) between our results and those reported by Hendsch and Tidor. Recently, Hendsch et al.<sup>45</sup> have also reported a good

agreement between the parameters used in this study (see Methods) and those used in their calculations.

Another method for studying protein hydration at high temperatures has recently been employed by Elcock and McCammon.<sup>22</sup> Utilizing a semi-empirical approach of fitting experimental data on changes in hydration free energies of charged and neutral residues as the temperature increases from 25°C to 100°C, they have derived temperature-dependent parameters which could be used to model changes in hydration free energies of proteins at high temperatures. Their approach involves estimation of both electrostatic and non-electrostatic terms. They have computed the free energies of folding for a few hyperthermophilic proteins including glutamate dehydrogenase. On the basis of these calculations, Elcock<sup>23</sup> concluded that hydration effects can stabilize hyperthermophilic proteins, and that the association of charged residues to form salt bridges may incur a lower desolvation energy penalty at high temperatures. Experimental estimates of the changes in hydration free energies of individual amino acids are ~1 Kcal/mol for an increase in temperature from 25°C to 100°C.<sup>22</sup> These results complement our calculations.

Hyperthermophilic proteins are required to control random conformational disorder due to higher entropy arising



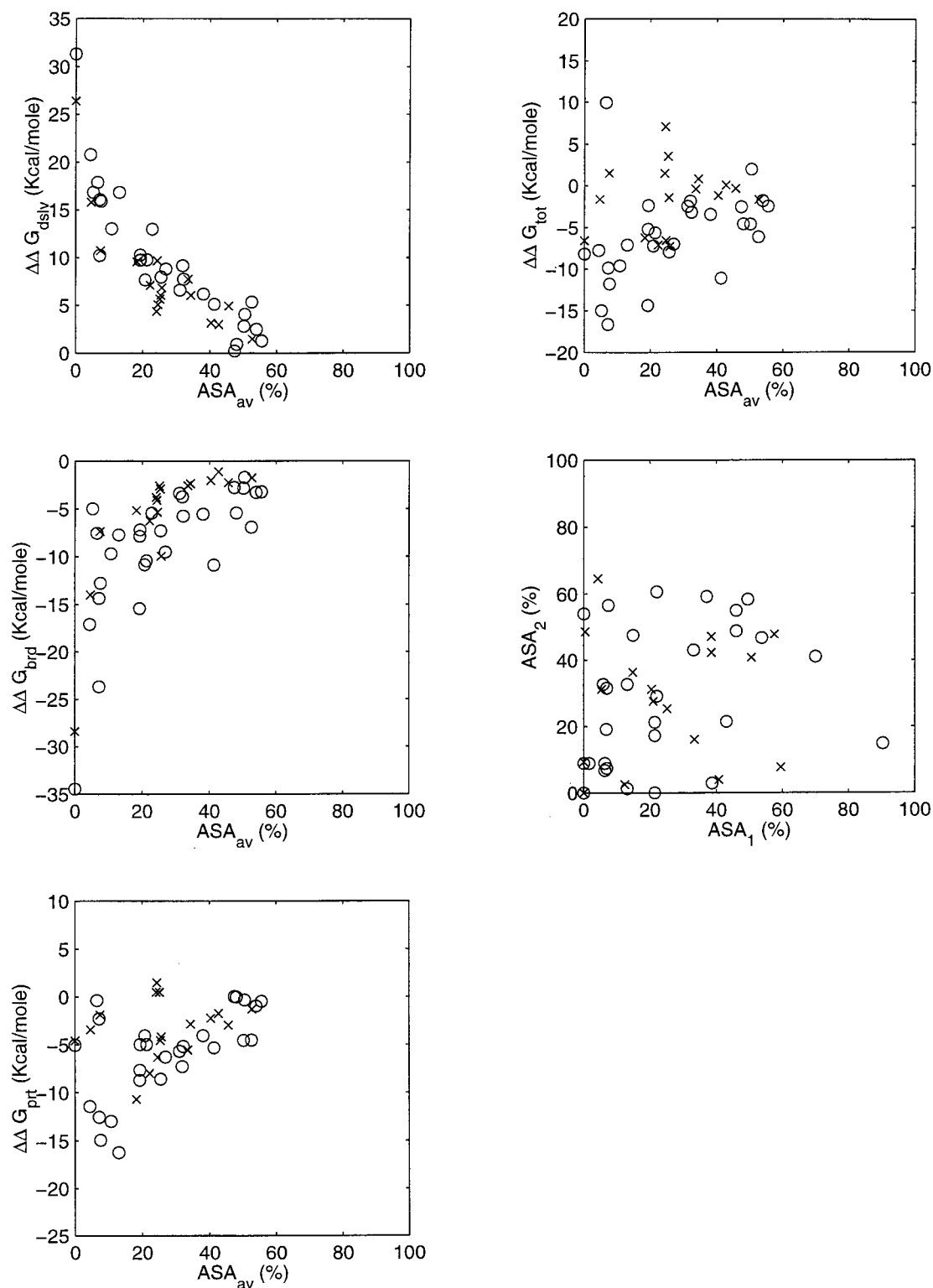


Fig. 4. Plots depicting relationship of various salt bridge energy terms with the location of salt bridges in the protein structure. Salt bridges from the thermophilic glutamate dehydrogenase (Chain B in 1GTM) are indicated by the symbol o, while an x indicates a salt bridge from the mesophilic glutamate

dehydrogenase (chain B of 1HRD).  $ASA_{av}$  stands for average accessible surface area computed from the individual accessible surfaces areas ( $ASA_1$  and  $ASA_2$ ) of the residues forming the salt bridge. A complete description of the energy terms is given in the Methods.

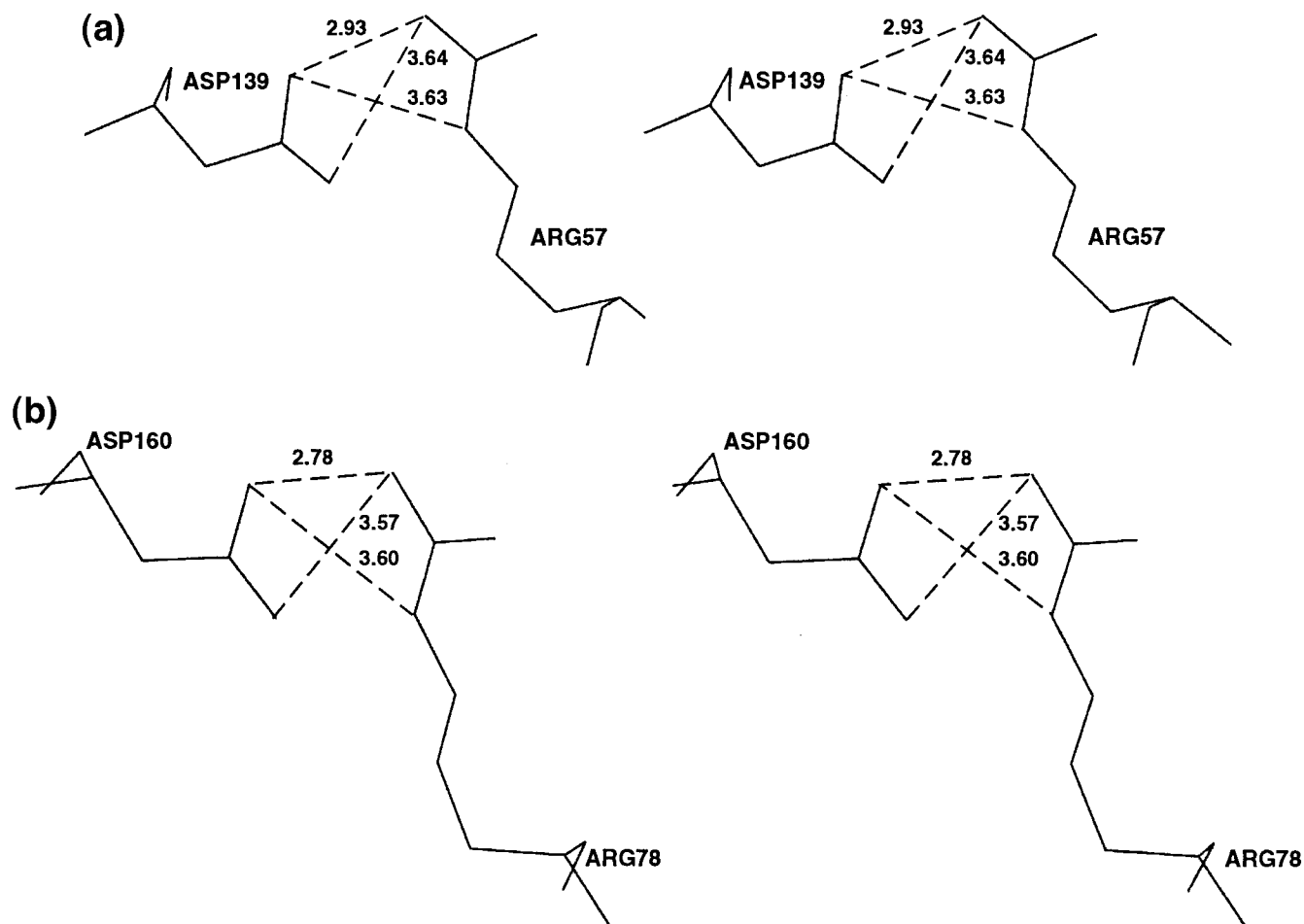


Fig. 5. A completely buried and spatially conserved salt bridge in (a) *Pyrococcus furiosus* glutamate dehydrogenase and (b) *Clostridium symbiosum* glutamate dehydrogenase. This salt bridge is highly stable in both

proteins even though it is completely buried. The stability of this salt bridge is due to the formation of hydrogen bonds between the side chains.

from the greater mobility of their constituent (groups of) atoms. If such a control had been missing, loss of protein function due to protein structure deformation or, even worse, due to protein unfolding may have ensued. This is critically important since chemical reaction rates also increase with temperature and even small conformational changes in, or nearby the active site can drastically alter catalysis. The structural plasticity in protein folds can be reduced by increasing the electrostatic interactions in the form of salt bridges and their networks. Once a thermophilic protein has folded, salt bridges and their networks can provide useful kinetic barriers resisting unfolding at high temperatures. Consistently, there are experimental indications that breaking a salt bridge involves overcoming a high conformational energy barrier.<sup>17</sup> Using site-directed mutagenesis, Kawamura et al.<sup>46</sup> have also observed that disruption of the salt bridge Glu34–Lys38 in the DNA binding protein HU from *Bacillus stearothermophilus* reduces its thermostability.

Recently, Xiao and Honig<sup>24</sup> have found that optimization of electrostatic interactions can enhance the electrostatic contribution to the stability of hyperthermophilic

proteins. They observed that electrostatic interactions are more favorable in the hyperthermophilic proteins. Furthermore, they observed that the electrostatic free energies of these proteins depend upon the location of the charges in the protein structure. Recently, we have analyzed electrostatic strengths of a large database (>220) of nonequivalent salt bridges from 36 nonhomologous monomeric proteins, whose high-resolution crystal structures are available in the PDB.<sup>30</sup> The electrostatic strength of a salt bridge depends upon its location in the protein, upon the orientation of the salt bridging side chains with respect to one another and the interaction of the salt bridge with the charges in the rest of the protein.<sup>47</sup> In the case of an isolated salt bridge, that is, when there are no charges in its vicinity, its electrostatic strength depends upon the balance between the desolvation penalty paid by the salt bridge and the orientation of the salt bridging side chains (salt bridge geometry). On the other hand, in the case of a networked salt bridge, neighboring charge(s) also affect the strength of the salt bridge. Frequently, the presence of neighboring charge(s) results in strengthening the interaction of the salt bridge with the rest of the protein (unpub-

lished results). Hence, networking stabilizes the salt bridges which are part of the network. This can be a good strategy for hyperthermophilic proteins to optimize their electrostatics, while conserving their hydrophobic cores. Results obtained by Xiao and Honig<sup>24</sup> and those presented in this paper appear to support this notion.

Within a monomer of the thermophilic PfGDH protein, on average, salt bridges and their networks appear to have a highly stabilizing electrostatic contribution. In contrast, the salt bridges in the monomer of the mesophilic CsGDH have only a marginally stabilizing electrostatic free energy. It is interesting to note that a conserved salt bridge between the monomers of CsGDH and PfGDH has a stronger stabilizing electrostatic free energy contribution in PfGDH. The change is larger than that expected on the basis of different optimal growth temperatures and solvent dielectric constants for *Pyrococcus furiosus* and *Clostridium symbiosum*. Moreover, while there are extensive networks of salt bridges in the monomer of PfGDH, they are conspicuously absent in the mesophilic protein CsGDH, particularly in the vicinity of the glutamate binding moiety. These networks not only provide extra stability to the electrostatic interactions in the thermodynamic sense, but can also provide kinetic barriers against protein deformation/melting or unfolding at higher temperatures. Xiao and Honig<sup>24</sup> have indicated that relative differences between electrostatic free energies may provide a useful insight into the contribution of electrostatic interactions toward protein thermostability. If we compare average values at room temperature for salt bridges between PfGDH and CsGDH (Tables III(a) and III(b)), we find that salt bridges in the thermophilic proteins are more stable by ~3 Kcal/mol. Most of this stability difference comes from the difference in the protein terms of PfGDH and CsGDH. The interaction of individual salt bridges with the rest of the protein is stronger in PfGDH than in CsGDH.

From the point of view of designing a thermostable protein starting from a mesophilic one, our results indicate that additional salt bridges should be engineered into the protein. However, engineering isolated salt bridges in different parts of the protein may not be as advantageous as clusters of salt bridges. Clustered salt bridges, and particularly engineered networks, may cooperatively enhance their stability. The region of choice for this engineering task may be a relatively flexible part of the protein, critical for protein function. The neighborhood of the protein active site may be a good candidate. It should be noted that the results presented here are based on the study of only a single thermophile–mesophile protein pair. Similar studies on other pairs are required, before the trends observed in this study can be generalized.

## ACKNOWLEDGMENTS

We thank Dr. Jacob Maizel for encouragement and helpful discussions. Dr. Dong Xu is thanked for guidance in getting started with DELPHI computations. We thank Dr. Bruce Tidor for further clarification of his paper, and for many useful comments. Dr. John Owens is thanked for help in preparing the figures. The personnel at FCRDC are

thanked for their assistance. The research of R. Nussinov in Israel has been supported in part by grant number 95-00208 from BSF, Israel, by a grant from the Ministry of Science by the Center of Excellence, administered by the *Israel Academy of Sciences*, by the Magnet grant, and by the Tel Aviv University Basic Research and Adams Brain Center grants. This project has been funded in whole or in part with Federal funds from the National Cancer Institute, National Institutes of Health, under contract number NO1-CO-56000. The content of this publication does not necessarily reflect the view or policies of the Department of Health and Human Services, nor does mention of trade names, commercial products, or organization imply endorsement by the U.S. Government.

## REFERENCES

1. Perutz MF. Stereochemistry of cooperative effects in haemoglobin. *Nature* 1970;228:726–739.
2. Barlow DJ, Thornton JM. Ion-pairs in proteins. *J Mol Biol* 1983;168:867–885.
3. Musafia B, Buchner V, Arad D. Complex salt bridges in proteins: statistical analysis of structure and function. *J Mol Biol* 1995;254:761–770.
4. Xu D, Tsai CJ, Nussinov R. Hydrogen bonds and salt bridges across protein-protein interfaces. *Protein Eng* 1997a;10:999–1012.
5. Xu D, Lin SL, Nussinov R. Protein binding versus protein folding: the role of hydrophilic bridges in protein associations. *J Mol Biol* 1997b;265:68–84.
6. Horovitz A, Fersht AR. Co-operative interactions during protein folding. *J Mol Biol* 1992;224:733–740.
7. Marqusee S, Sauer RT. Contribution of a hydrogen bond/salt bridge network to the stability of secondary and tertiary structures in lambda repressor. *Protein Sci* 1994;3:2217–2225.
8. Pervushin K, Billeter M, Siegel G, Wuthrich K. Structural role of a buried salt bridge in the 434 repressor DNA-binding domain. *J Mol Biol* 1996;264:1002–1012.
9. Lounnas V, Wade RC. Exceptionally stable salt bridges in cytochrome P450cam have functional roles. *Biochemistry* 1997;36:5402–5417.
10. Singh UC. Probing the salt bridge in the dihydrofolate reductase-methotrexate complex by using the coordinate-coupled free energy perturbation method. *Proc Natl Acad Sci USA* 1988;85:4280–4284.
11. Serrano L, Horovitz A, Avron B, Bycroft M, Fersht AR. Estimating the contribution of engineered surface electrostatic interactions to protein stability by using double mutant cycles. *Biochemistry* 1990;29:9343–9352.
12. Barril X, Aleman C, Orozco M, Luque FJ. Salt bridge Interactions: stability of ionic and neutral complexes in the gas phase, in solution and in proteins. *Proteins* 1998;32:67–79.
13. Sun DP, Sauer U, Nicholson H, Matthews BW. Contributions of engineered surface salt bridges to the stability of T4 lysozyme determined by directed mutagenesis. *Biochemistry* 1991;30:7142–7153.
14. Dao-pin S, Anderson DE, Baase WA, Dahlquist FW, Matthews BW. Structural and thermodynamic consequences of burying a charged residue within the hydrophobic core of T4 lysozyme. *Biochemistry* 1991;30:11521–11529.
15. Hendsch ZS, Tidor B. Do salt bridges stabilize proteins? A continuum electrostatic analysis. *Protein Sci* 1994;3:211–226.
16. Waldburger CD, Schildbach JF, Sauer RT. Are buried salt bridges important for protein stability and conformational specificity? *Nat Struct Biol* 1995;2:122–128.
17. Waldburger CD, Jonsson T, Sauer RT. Barriers to protein folding: formation of buried polar interactions is a slow step in acquisition of structure. *Biochemistry* 1996;35:2629–2634.
18. Honig BH, Hubell WL. Stability of “salt bridges” in membrane proteins. *Proc Natl Acad Sci USA* 1984;81:5412–5416.
19. Querol E, Perez-Pons JA, Mozo-Villarias A. Analysis of protein conformational characteristics related to thermostability. *Protein Eng* 1996;9:256–271.

20. Kumar S, Tsai CJ, Ma B, Nussinov R. Contribution of salt bridges toward protein thermostability. *J. Biomol Struct Dyn* 1999; in press.
21. Yip KSP, Stillman TJ, Britton KL, et al. The structure of *Pyrococcus furiosus* glutamate dehydrogenase reveals a key role for ion-pair networks in maintaining enzyme stability at extreme temperatures. *Structure* 1995;3:1147–1158.
22. Elcock AH, McCammon JA. Continuum solvation model for studying protein hydration thermodynamics at high temperatures. *J Phys Chem B* 1997;101:9624–9634.
23. Elcock AH. The stability of salt bridges at high temperatures: implications for hyperthermophilic proteins. *J Mol Biol* 1998;284:489–502.
24. Xiao L, Honig B. Electrostatic contributions to the stability of hyperthermophilic proteins. *J Mol Biol* 1999;289:1435–1444.
25. Yip KSP, Britton KL, Stillman TJ, et al. Insights into the molecular basis of thermal stability from the analysis of ion pair networks in the glutamate dehydrogenase family. *Eur J Biochem* 1998;255:336–346.
26. Robb FT, Park JB, Adams MWW. Characterization of an extremely thermostable glutamate dehydrogenase: a key enzyme in the primary metabolism of hyperthermophilic archaeobacterium *Pyrococcus furiosus*. *Biochim Biophys Acta* 1992;1120:267–272.
27. Klump H, DiRuggiero J, Kessel M, Park JB, Adams MWW, Robb FT. 1992. Glutamate dehydrogenase from the hyperthermophile *Pyrococcus furiosus*. Thermal denaturation and activation. *J Biol Chem* 1992;267:22681–22685.
28. Baker PJ, Britton LK, Engel PC, et al. Subunit assembly and active site location in the structure of glutamate dehydrogenase. *Proteins* 1992;12:75–86.
29. Stillman TJ, Baker PJ, Britton LK, Rice DW. Conformational flexibility in glutamate dehydrogenase. Role of water in substrate recognition and catalysis. *J Mol Biol* 1993;234:1131–1139.
30. Bernstein F, Koetzle T, Williams G, et al. The Protein data bank: a computer based archival file for macromolecular structures. *J Mol Biol* 1977;112:535–542.
31. Lee BK, Richards FM. The interpretation of protein structures. Estimation of static accessibility. *J Mol Biol* 1971;55:379–400.
32. Tsai CJ, Nussinov R. Hydrophobic folding units derived from dissimilar monomer structures and their interactions. *Protein Sci* 1997;6:24–42.
33. Gilson MK, Rashin A, Fine R, Honig B. On the calculation of electrostatic interactions in proteins. *J Mol Biol* 1985;183:503–516.
34. Gilson MK, Sharp KA, Honig BH. Calculating the electrostatic potential of molecules in solution: method and error assessment. *J Comp Chem* 1988;9:327–335.
35. Gilson MK, Honig BH. Calculation of the total electrostatic energy of a macromolecular system: Solvation energies, binding energies, and conformational analysis. *Proteins* 1988;4:7–18.
36. Sharp KA, Honig B. Electrostatic interactions in macromolecules: theory and applications. *Annu Rev Biophys Biophys Chem* 1990;19:301–332.
37. Honig B, Sharp K, Yang A. Macroscopic models of aqueous solutions: biological and chemical applications. *J Phys Chem* 1993;97:1101–1109.
38. Sitkoff D, Sharp KA, Honig B. Accurate calculation of hydration free energies using macroscopic solvent models. *J Phys Chem* 1994;98:1978–1988.
39. Radzicka A, Wolfenden R. Comparing the polarities of the amino acids: side chain distribution coefficients between the vapor phase, cyclohexane, 1-octanol and neutral aqueous solution. *Biochemistry* 1988;27:1664–1670.
40. Gilson MK, Honig BH. Calculation of electrostatic potential in an enzyme active site. *Nature* 1987;330:84–86.
41. Klapper I, Hagstrom R, Fine R, Sharp K, Honig B. Focusing of electric fields in the active site of Cu-Zn superoxide dismutase: effects ionic strength and amino acid modification. *Proteins* 1986;1:47–59.
42. Lide DR, Editor. *CRC Handbook of chemistry and physics*. 79<sup>th</sup> Edition. Boca Raton: CRC Press. 1998–1999.
43. Tsai CJ, Lin SL, Wolfson H, Nussinov R. A dataset of protein-protein interfaces generated with a sequence order independent comparison technique. *J Mol Biol* 1996;260:604–620.
44. deBakker PIW, Hunenberger PH, McCammon JA. Molecular dynamics simulations of the hyperthermophilic protein Sac7d from *Sulfolobus acidocaldarius*: contribution of salt bridges to thermostability. *J Mol Biol* 1999;285:1811–1830.
45. Hendsch ZS, Sindelar CV, Tidor B. Parameter dependence in continuum electrostatic calculations: a study using salt bridges. *J Phys Chem B* 1998;102:4404–4410.
46. Kawamura S, Tanaka I, Kimura M. Contribution of a salt bridge to the thermostability of DNA binding protein HU from *Bacillus stearothermophilus* determined by site directed mutagenesis. *J Biochem* 1997;121:448–455.
47. Kumar S, Nussinov R. Salt bridge stability in monomeric proteins. *J Mol Biol* 1999;293:1241–1255.